

# MAGNETIC IMAGING OF FCC FEEDSTOCKS TO MODEL ASPECTS OF THEIR CRACKING KINETICS AND PRODUCT SLATES

P.S. Virk

Department of Chemical Engineering  
M. I. T., Cambridge, MA 02139

**KEYWORDS:** Magnetic Resonance, Catalytic Cracking, Modelling.

## INTRODUCTION

**Motivation.** This work reports on a system for the Magnetic Imaging of FCC Feedstocks, acronym MIFF, that is being devised to model the fundamental chemical aspects of their cracking kinetics and product slates. It is motivated by the need to engineer, and predict the performance of, fluidized cat crackers using modern catalysts to crack ever heavier feeds at ever increasing reaction severities and gasoline selectivities under ever closer environmental scrutiny. NMR imaging adds a unique dimension to FCC feed characterization because of its intimate relation to molecular topology. Thus acid catalysts can crack virtually all the C-C bonds in hydrocarbons except those either within or adjacent to aromatic rings and NMR can directly detect these uncrackable sp<sup>2</sup>-hybridized aromatic core carbons and their adjacent sp<sup>3</sup> benzylic carbons, providing the asymptotic extent to which a feedstock can be cracked and proffering insights into the structures of the product fragments.

**Background.** Of the voluminous literature on NMR applied to hydrocarbon mixtures, the present work has most been influenced by the classic papers of Knight (1967), Shoolery and Budde (1976) and Deutsche, Jancke and Zeigan (1976), specific articles by Ladner and Snape ((1978), Gillet et al (1981), Netzel et al (1981), and especially Cookson and Smith (1985, 1987), and the texts by Stothers (1972), Breitmaier and Voelter (1987) and Croasmun and Carlson (1994). Earlier efforts relevant to FCC feeds include Bouquet and Bailleul (1986), who used the methods of Cookson and Smith (1985) to assay carbons by their attached protons; Mauleon et al (1987), who devised a coke factor from carbon aromaticity; and a recent note based on the present work (Kim et al 1998) which applied NMR to enhance conventional and mass spectrometric characterizations.

## MIFF SYSTEM

Figure 1 schematically depicts the three facets of the MIFF system, sample preparation, NMR experiments, and data analysis. In sample preparation, internal standards are gravimetrically incorporated into the FCC feedstock oils, typically VGOs and ATBs, to enable precise analysis and interpretation of the NMR experiments. Three internal standards are used, namely, deuteriochloroform CDCl<sub>3</sub>, as oil solvent and spectrometer lock; dioxane, C<sub>4</sub>H<sub>8</sub>O<sub>2</sub>, abbr DIOX, to assist in spectral integrations; and tetramethylsilane, Si(CH<sub>3</sub>)<sub>4</sub>, abbr TMS, as a spectral frequency reference. The primary NMR experiments performed provide quantitative C13 and H1 spectra, the spectral regions and individual resonances observed therein being identified and interpreted by additional 1-D and 2-D procedures that include DEPT, COSY, HETCOR, and HMQC. Spectral data are analysed in two trains, according to either their integral regions, abbr IR, or their canonical groups, abbr CG. In the IR train, the observed spectra are parsed into more or less coarse regions, each comprising chemically similar sorts of atoms. The IR train accounts for 100% of feedstock atoms and provides useful overall parameters, such as the percent of feedstock atoms, either carbon or hydrogen, that are aromatic. In the CG train, certain groups of spectral peaks that arise from atoms belonging to particular molecular moieties are recognized, particularly those in n-alkane straight chains and in 2-, 3-, 4-, 5-, and interior-methyl alkane branched chains. The CG train thus provides high-level quantitative information about certain molecular species; however the sum of identified species is but a fraction of the total, typically amounting to ~ 40% of feedstock atoms. Outputs from the coarse but complete IR train and the fine but fractional CG train are shown in the bottom row of Figure 1. The IR train provides carbon and hydrogen aromaticities, as well as more detailed regional data, and thence hydrogen atom counts, and thermochemical information. The CG train detects n-alkane content and chain length, as well as the contents of a variety of methyl-alkane moieties. Both trains are combined to form a set of NMR groups that characterize the feedstock.

## NMR EXPERIMENTS

**13-C.** Figure 2 shows the 13-C NMR spectrum of a VGO feedstock called V2 in Table 1 (infra). The position of a peak on the x-axis, its resonance frequency or chemical shift, c, in units of ppm relative to TMS, is indicative of C atom type, while peak height on the y-axis, its absorption intensity, i, with arbitrary units, is roughly proportional to the abundance of such C atoms in the sample. Precise carbon atom amounts are obtained from peak integration, these integrals being the five continuously increasing stepped segments in the figure, their c-domains and magnitudes being noted below the abscissa. The major spectral regions observed are:

Region	c (range)	C-atom type
TMS	0.0	methyl carbons in TMS
Cal	10 - 52	aliphatic carbons in feedstock, sp <sup>3</sup> hybridized
DIOX	~67	methylene carbons in DIOX
CDCl <sub>3</sub>	~78 triad	C in CDCl <sub>3</sub> solvent
Car	112 - 150	aromatic carbons in feedstock, sp <sup>2</sup> hybridized

The wide separation between the regions of aliphatic and of aromatic carbons is noteworthy, allowing unambiguous delineation of these two broad categories; the integrals corresponding to these regions provide the carbon aromaticity  $Car = 16.8\%$ . Further demarcations shown below the spectrum, called Cumulative Integral Regions, sort carbon atoms into categories with the following approximate chemical interpretations: Carqt is aromatic quaternary, which are inherently of two kinds, either fused ring junction or substituted, not distinguished here; Carpi and Carpo are both aromatic protonated, the i and o being subtle distinctions between them; the sum  $Car(qt+pi+po) = Car$ . Among aliphatic carbons, Calhs is aliphatic highly substituted, Calbr is aliphatic branched (single substitution, such as methyl), Calch is aliphatic chains, mainly CH<sub>2</sub>, and Calme is aliphatic methyls, all CH<sub>3</sub>. Many additional individual spectral regions can be distinguished in Figure 2, and these have been labelled beside their principal peaks as follows: Regions B, D, H, and G (two tall peaks at  $c \sim 30$ ) respectively contain the carbon atoms C1, C2, C3, and (C4, C25) in linear n-alkane chains. Region C contains mainly methyl groups, pendant on a variety of alkane, cyclo-alkane and aromatic structures. Regions E and F contain carbon atoms in C5- and C6-cyclo-alkane rings, as well as C2 in 2-methyl-alkanes. Regions A, I, J and K contain carbon atoms from branched (iso-) alkanes. Peaks of the n-alkane moiety in regions B, D, H, and G, called a Canonical Group, reveal the present VGO to possess an n-alkane chain content of 17.1 C atoms per 100 C atoms of feedstock, with an average chain length  $L = 7.8$ , that is, for every set of terminal n-alkane atoms (C1, C2, C3), there are 4.8 interior n-alkane atoms (C4, C25).

**1-H.** Figure 3 shows the 1-H NMR spectrum of VGO feedstock V2. The x-axis is resonance frequency, or chemical shift,  $h$ , in units of ppm relative to TMS, indicative of hydrogen type, while the y-axis is absorption intensity,  $i$ , with arbitrary units, approximately proportional to the abundance of such hydrogen atoms in the sample. Accurate hydrogen amounts are obtained from integrals of peak intensities, seen as four continuous stepped lines in the figure, their h-domains and numerical magnitudes noted below the abscissa. The 1-H spectrum has the following regions:

Region(s)	$h$ (range)	H-atom type
TMS	0.0	H in methyls of TMS
Hgam, Hbet, Hbzy	0.4 - 3.2	aliphatic H, attached to sp <sup>3</sup> hybridized C atoms
DIOX	~3.65	H in methylenes of DIOX
Har	6.5 - 9.2	aromatic H, attached to sp <sup>2</sup> hybridized ring C atoms

The wide separation between the regions of aliphatic and of aromatic hydrogens is noteworthy, permitting their unambiguous delineation, and providing the hydrogen aromaticity  $Har = 4.1\%$ . The Cumulative Integral Regions, shown below the spectrum, have the following approximate chemical interpretations. The aromatic H region is subdivided into Hart, Hard, and Harm, with sum  $Har(t+d+m) = Har$ ; of these, Harm contains H atoms from all aromatic rings; Hard contains H atoms from  $\geq 2$ - but not from 1-ring aromatics; and Hart contains H atoms from  $\geq 3$ - but not from  $\leq 2$ -ring aromatics. Next, Hbzy are benzylic H atoms, attached to aliphatic C atoms bonded to aromatic rings; Hbzy thus reflects the degree of aromatic ring substitution. Of the two broad benzylic peaks in the spectrum,  $\alpha 1$  is mainly H atoms on methyls pendant on mono-aromatic rings, while  $\alpha 2$  contains a host of other benzylic hydrogens. Hbet are H atoms attached to aliphatic C atoms bonded to other aliphatic C atoms; region Hbeta, with huge peak  $\beta 1$ , is primarily H atoms in the methylene CH<sub>2</sub> units of alkyl chains, while Hbetb includes H atoms on CH (methine) and CH<sub>2</sub> (methylene), the peaks  $\beta 1$ ,  $\beta 2$  including H atoms on alicyclic rings. Hgam, with large twin peaks  $\gamma$ , are H atoms in aliphatic methyls CH<sub>3</sub>.

**2-D HETCOR.** Figure 4 is a 2-dimensional contour plot showing the islands in an H-C atom correlation spectrum of VGO feedstock V2. The HETCOR experiment, described by Gray (1994), is the equivalent of recording full 1-H spectra, such as shown in Figure 3, at each of a myriad slices of a 13-C spectrum, such as shown in Figure 2. A correlation island at chemical shift coordinates  $[c, h]$  represents a carbon of shift  $c$  connected to a hydrogen of shift  $h$ , with island cross-section (actually, its peak height and volume) crudely related to the abundance of the correlated atoms in the feedstock. In Figure 4, with abscissa (F2 axis)  $c$  and ordinate (F1 axis)  $h$ , the large lens-shaped island #3 at coordinates  $[c, h] = [14.2, 0.89]$  arises from the H and C atoms in the terminal methyl group of an n-alkane chain and is so labelled. Numerous other islands are also visible in the figure, with those that have been chemically identified being labelled in three rows respectively representing methyl CH<sub>3</sub>, methylene CH<sub>2</sub>, and methine CH carbons. Identified islands belong to the following Canonical Groups: n-alkane (C1, C2, C3, C4, C25), 2-methyl alkane (C1, C2, C3), 3-methyl alkane (C1, Me, C3), 4-methyl alkane (C1, C3), and interior-methyl alkane (Me, Cj(unction)). The present HETCOR spectrum had a dynamic range, that is, the ratio of tallest peak height/noise level, of 615, and the 30 islands in Figure 4 resulted from a contour threshold about 3 times higher than the noise level. Decreasing the threshold to 1.5 times noise resulted in 58 islands, of which 23 could be identified, revealing the additional moieties: 4-methyl alkane (C1, C2, C3, C4), 5-methyl alkane (C2, C4), interior-methyl alkane, including phytyl, (Me, Cj, Cj+1, Cj+2, Cj+3), alkyl-cyclo-C6-alkane (Me, Cr(ing)), and alkyl-benzene (C3).

## RESULTS

Table 1 presents data from both conventional and MIFF characterizations of six representative FCC feeds, four VGOs V1 to V4 and two ATBs A1 and A2.

Conventional properties include gravity, Conradson carbon residue, and elemental assays of H, C, S, N, from which H elem, H atoms/100 C atoms, has been calculated.

MIFF data, from top to bottom, show results from the IR and CG trains; for samples run in duplicate, average values and an estimate of their experimental uncertainty are both quoted. Among IR train C13

data, the two rows labelled diox/oil are the ratios of carbon atoms in the dioxane internal standard to those in the oil; the gravimetric row was calculated from sample preparation and elemental assays while the spectral row is independently derived from the regional integrals of the experimental spectra. Agreement between these internal standard ratios is a stringent test of C13 NMR data fidelity. The next row, Car, and then the next seven rows, called CIRs for Cumulative Integral Regions, provide a breakdown of feedstock carbon atom types, as percentages. CIRs are so named because each is the accumulation of Detailed Integral Regions, DIRs, which represent the finest parsing of spectral integrals. The chemical significance of Car and the CIRs was earlier considered in connection with the 13-C NMR spectrum in Figure 2. The last row, H count, H / 100 C, is derived from the DIRs by summing the products of DIR amount times the number of H atoms per C atom of the type contained therein. Data from the IR train H1 are analogous to those from the IR train C13, with two diox/oil rows, gravimetric and spectral, followed by Har and then seven CIRs, whose chemical significance was earlier considered with the 1-H NMR spectrum in Figure 3. Finally, the first row of the CG Train C13 provides the average chain length of n-alkane moieties in the feedstock, Lna in C atoms. The second and third rows of the CG train respectively provides the percentages of C atoms in n-alkane moieties Cna, and in methyl-alkane moieties Cma, the latter comprising 2-, 3-, 4-, 5-, and interior-methyl substituted alkane chains. These are used, along with Car from the IR train, shown again in the fifth row, to form a final set of 4 NMR-derived canonical groups for each feedstock. The group Ccs in the fourth row, comprising cyclic and highly substituted aliphatic C atoms, is a (large) remnant obtained from  $Ccs = 100 - Cna - Cma - Car$ .

**Dioxane/Oil Ratios.** Figure 5 compares the internal standard ratios of dioxane to oil D/O,g from the gravimetric sample preparation procedure to those derived from spectral integration D/O,s. Data from C13 and H1 spectra are respectively differentiated by large solid and small hollow symbols in the plot and by suffixes c and h in the legend. Linear regression of these data, shown by the dashed line in the figure, yields:

$$(E1) \quad D/O,s = (0.00 \pm 0.01) + (1.08 \pm 0.06) D/O,g.$$

The present NMR integral measurements are accurate to within 8% absolute, with a precision of  $\pm 6\%$  relative to one another. Such quantitative fidelity is a tribute to modern NMR spectrometers, which can evidently excite and detect diverse kinds of C and H atoms in the feedstock over wide frequency ranges on both sides of the C and H atoms in the dioxane internal standard.

**MIFF Maps.** MIFF data in Table 1 provide an aromaticity map, Car vs Har, and an n-alkane chain map, Cna vs Lna, of relevance to FCC performance as discussed in the next section. The aromaticity map showed Har  $\approx 0.3$  Car, from which, using feedstock H content  $\approx 172$  H/100 C, there are typically 51 aromatic H atoms/100 aromatic C atoms, that is, 51% of the aromatic carbons are protonated. The other 49% of the aromatic carbons must therefore be quaternary, and from the benzylic H atoms we estimate 19% of these to be substituted, so the remaining 30% are fused, at ring junctions. The n-alkane chain map showed that VGO and ATB feedstocks typically possess  $[Cna, Lna] = [17 \pm 3, 9 \pm 1]$ , with the highest observed content Cna = 40 and the longest L = 12.

**Carbon Atom Groups.** The upper panels of Figure 6 present NMR-derived carbon atom groups as pie charts for feedstocks A1 and V4. Each pie has four slices [Cna, Cma, Ccs, Car], respectively the percentages of n-alkane, methyl-alkane, alicyclic + highly substituted, and aromatic carbon atoms in the feedstock. The variations in pie slices between A1 and V4, the former containing more n-alkanes and possessing the lower aromaticity, anticipate differences between their performances in FCC units. By way of comparison, the lower panels of Figure 6 show mass spec-derived data for each of A1 and V4, using the high-resolution electron impact methods described by Fisher (1986, 1990). Mass spec data are compressed into four groups of decreasing Z-numbers [Wpar, Wcyp, Wmono, Wdih], respectively the weight percentages of paraffins, n- and iso- (Z = 2), cyclo-paraffins, mono-, di-, tri- and higher ( $0 \geq Z \geq -4$ ), mono-aromatics (Z = -6), and di- and higher-aromatics (Z  $\leq -8$ ). The preceding characterizations differ fundamentally in that NMR distinguishes individual atoms by their bonding environment, without regard for the host molecules they inhabit, whereas mass spectrometry distinguishes whole molecules within homologous series of formula  $C_nH_{2n+Z}$ . By joint use of the MIFF and mass spec pies we can ascertain (Wmono + Wdih - Car), the aliphatic carbons associated with the aromatic core carbons, which respectively amount to 16% and 29% for A1 and V4, rather larger than Car itself. The methyl-alkane group Cma of MIFF has no analogue in mass spec data because the latter does not distinguish n- from iso-paraffins, both having the same Z = 2. Finally, it is curious that, despite their different chemical origins, the n-Alkane content Cna from MIFF and the paraffin content Wpar from the mass spec are numerically within  $\pm 2\%$  of one another for each of A1 and V4, and this rough equality between Cna and Wpar also holds for all the other oils in Table 1.

## MODELLING FCC PERFORMANCE

**Theoretical Basis.** Figure 7 depicts the possible relation of our NMR-derived characterizations of a feedstock to its FCC performance, comprising conversion kinetics and products, using data for oil V4. MIFF groups [Cna, Cma, Ccs, Car] = [19.7, 8.8, 54.2, 17.4] are shown in the uppermost ribbon, with segments proportional to their respective abundances. IR train H1 data were used to slightly elaborate Car and Ccs, with aromatic core C atoms classified by their ring sizes, mono-, di-, and tri-+higher, and the benzylic C atoms pendant upon such rings shown as a (small) subset of Ccs. The kinetics of cracking the MIFF groups under acid-catalysed conditions with carbenium ion intermediates are depicted in the

second ribbon from the top, based on the works of Nace (1969), Venuto & Habib (1979), and Pines (1981). N-alkane chains, comprising mainly secondary carbons, are amenable to acid cracking, but with modest kinetics that are further a function of chain length; methyl-alkanes and most of the alicyclic + substituted group crack rapidly, on account of reactive tertiary carbons within them; the entire aromatic core group and the benzylic portion of the Ccs group are not cracked at all. The third ribbon depicts potential products from complete conversion of the feedstock by acid-catalysed cracking only. Gas + gasoline products arise from n-alkanes, methyl-alkanes, alicyclic + substituted carbons excluding the benzylic di- and tri- segments, and mono-aromatics. Light cycle oil LCO is related to the di-aromatic group and to the benzylic carbons attached to di-aromatics, while decant oil + coke DO+C is associated with tri- and higher aromatics and their benzylic carbons. For the present feedstock V4, MIFF data provide potential product yields of  $[GG^*, LCO^*, DO+C^*] = [85.4, 6.7, 7.9] C/100 C$ . Actual product yields from FCC of V4 at commercial conditions are shown in the bottom ribbon, being [Gas, Gasoline, LCO, DO, Coke] = [20.4, 43.7, 19.2, 11.6, 5.1] wt%. The actual yield of gas + gasoline = 64.1 is appreciably lower than the asymptotic maximum  $GG^* = 85.4$  inferred from MIFF, with the actual yields of LCO and DO+Coke correspondingly higher than the asymptotic  $LCO^*$  and  $DO+C^*$ . These differences reflect both kinetic constraints on conversion as well as the operation of additional catalytic reaction paths, such as hydrogen transfer and polymerization, in parallel with the dominant acid cracking path.

**Decant Oil + Coke Yields.** As an example of how MIFF parameters might be employed to model the yields of FCC products, Figure 8 is a 3-dimensional plot of observed DO+Coke yields, wt%, on a MIFF aromaticity map of Har, H/100 H vs Car, C/100 C. The data can be seen to ascend from the origin at near lower left roughly along a diagonal toward the far upper right. A projection of the observed relationship on the x-z plane reveals that  $DO+C \approx 0.9 Car$ , about twice as large as the theoretically expected from the parameter  $DO+C^*$  computed in Figure 7.

**Overall Cracking Kinetics.** The overall kinetics of feedstock conversion in the riser of an FCC unit have been considered by Weekman & Nace (1970) whose model, with Voorhies' (1945) expression for coke deposition on the catalyst, can be used to derive the overall cracking rate constant  $k_0$  from operating conditions and observed conversions. The observed  $k_0$  are then normalized to standard residence time  $\tau$  and temperature  $T$  K to provide an apparent cracking rate constant  $k_0^*$  characteristic of the feedstock. Figure 9 is a 3-D plot of  $k_0^*$  on a MIFF n-alkane chain map of  $Lna, C$  atoms, vs  $Cna, C/100 C$ , for four FCC feeds, two each VGOs and ATBs, that possessed roughly the same specific gravities,  $SG = 0.903 \pm 0.004$ , and carbon aromaticities  $Car = 15 \pm 1$ . Three of these feeds, with chain lengths  $8.6 \leq Lna \leq 10.1$  and n-alkane contents  $18 \leq Cna \leq 40$ , exhibit  $k_0^* \approx 0.15$ , whereas the fourth, with  $Lna = 10.6, Cna = 33$  has an appreciably lower  $k_0^* = 0.10$ . These data imply that feedstock conversion kinetics may be retarded by n-alkane chains longer than a critical  $Lna^* \approx 10.3$ . More extensive data are needed to verify and define a critical ( $Lna^*, Cna^*, k_0^*$ ) surface for kinetic retardation, though it is interesting that Nace (1969) reported the cracking kinetics of pure n-alkanes to reach a maximum at  $Lna = 8$  (hexadecane) and then decline for longer chains.

**ACKNOWLEDGEMENTS:** This work was initiated and supported by Larry Hallee, late of the Stone & Webster Engineering Corporation, Houston, TX. The author is indebted to Jeanne Owens of the MIT Spectrometry Laboratory, for help with NMR spectra, as well as Mike Silverman and Atulya Saraf of Stone & Webster, for discussions of Mass Spec and FCC.

## REFERENCES

- Knight, S.A.: Chem. Ind., 1920-1923 (1967).  
 Shooley, J.N.; Budde, W.L.: Anal. Chem., **48**, 1458-1461 (1976).  
 Deutsch, K.; Jancke, H.; Zeigan, D.: J. Prakt. Chem. Ind., **318**, 177-184 (1976).  
 Ladner, W.R.; Snape, C.E.: Fuel, **57**, 658-662 (1978).  
 Gillet, S.; Rubini, P.; Delpuech, J.J.; Escalier, J.C.; Valentin, P.: Fuel, **60**, 221-225 (1981).  
 Gillet, S.; Rubini, P.; Delpuech, J.J.; Escalier, J.C.; Valentin, P.: Fuel, **60**, 226-230 (1981).  
 Netzel, D.A.; McKay, D.R.; Heppner, R.A.; Guffey, F.D.; Cooke, S.D.; Varie, D.L.; Linn, D.E.: Fuel, **60**, 307-320 (1981).  
 Cookson, D.J.; Smith, B.E.: Anal. Chem., **57**, 864-871 (1985).  
 Cookson, D.J.; Smith, B.E.: Energy & Fuels, **1**, 111-120 (1987).  
 Stothers, J.B.: "Carbon-13 NMR Spectroscopy", Academic Press, New York, NY 1972.  
 Breitmaier, E.; Voelter W.: "Carbon-13 NMR Spectroscopy: High-Resolution Methods and Applications", 3rd Ed., VCH Publishers, Weinheim, Germany, 1987, pp73-105.  
 Croasmun, W.R.; Carlson, R.M.K.: "Two-Dimensional NMR Spectroscopy: Applications for Chemists and Biochemists", 2nd Ed., VCH Publishers, Weinheim, Germany, 1994.  
 Bouquet, M.; Bailleul, A.: Fuel, **65**, 1240-1246 (1986).  
 Mauleon, J.L.; Sigaud, J.B.; Biedermann, J.M.; Heinrich, G.: Proc. 12th World Petroleum Congress, Houston TX, [18], 1-7, Wiley, London (1987).  
 Kim, H.N.; Verstraete, J.J.; Virk, P.S.; Fafet, A.: Oil & Gas J., **96** (37) 85-88 (1998).  
 Gray, G.A., Ch 1, pp 46-49 in Croasmun, W.R.; Carlson, R.M.K.: "Two-Dimensional NMR Spectroscopy: Applications for Chemists and Biochemists", 2nd Ed., VCH Publishers, Weinheim, Germany (1994).  
 Fisher, I.P.: Fuel, **65**, 473-479 (1986).

- Fisher, I.P.: Appl. Catalysis, **65**, 189-210 (1990).  
 Nace, D.M.: Ind. Eng. Chem., Prod. Res. Dev., **8**, 31 (1969).  
 Venuto, P.B.; Habib, E.T.: "Fluid Catalytic Cracking with Zeolite Catalysts", Marcel Dekker, Inc., New York, (1979).  
 Pines, H.: pp1-122 in "The Chemistry of Catalytic Hydrocarbon Conversions", Academic Press, New York, (1981).  
 Weekman, V.W.; Nace, D.M.: A.I.Ch.E. J., **16**, 397-404 (1970).  
 Voorhies, A.: Ind. Eng. Chem., **37**, 318 (1945).

**TABLE I. Conventional and MIFF Characterizations of Representative FCC Feedstocks.**

Oil		V1	V2	A1	A2	V3	V4
<b>CONV DATA</b>							
API	deg	26.8	24.0	25.5	25.1	20.6	23.4
SG	15.6C	0.894	0.910	0.901	0.903	0.930	0.914
CCR	wt%	-	-	2.62	2.96	0.42	0.27
<b>Elemental Assay</b>							
H	wt%	12.91	12.50	12.94	12.54	12.14	12.47
C		86.63	86.28	86.60	87.08	85.52	86.65
S		0.44	1.03	0.50	0.28	2.22	0.98
N		-	0.19	0.20	-	0.20	0.11
H elem	H/100 C	177.6	172.6	178.0	171.6	169.1	171.5
<b>MIFF DATA</b>							
<b>IR Train C13</b>							
diox/oil	gravimetric	0.116	0.114	0.141 ± 0.000	0.141	0.024 *	0.143
diox/oil	spectral	0.113	0.104	0.156 ± 0.000	0.151	0.027 *	0.163
Car	C/100 C	12.5	16.8	14.8 ± 0.6	15.8	24.9 ± 0.7	17.4 ± 0.1
<b>CIRs</b>							
Carqt		5.4	7.5	6.6 ± 0.0	7.8	12.6 ± 0.9	8.2 ± 0.6
Carpi		1.8	2.3	1.9 ± 0.0	2.5	3.4 ± 0.1	2.4 ± 0.2
Carpo		5.3	7.0	6.3 ± 0.5	5.5	8.9 ± 0.3	6.8 ± 0.7
Calhs		7.5	7.5	2.9 ± 0.2	4.4	5.1 ± 0.0	6.8 ± 0.9
Calbr		18.9	17.9	13.2 ± 0.2	16.7	15.2 ± 0.5	18.4 ± 0.5
Calch		45.6	42.7	58.3 ± 0.2	51.5	38.7 ± 0.4	43.8 ± 1.2
Calme		15.6	15.1	10.8 ± 0.0	11.6	16.1 ± 0.3	13.7 ± 0.1
H count	H/100 C	182.1	173.6	178.9 ± 0.4	174.3	164.6 ± 1.1	171.7 ± 0.3
<b>IR Train H1</b>							
diox/oil	gravimetric	0.130	0.132	0.159 ± 0.000	0.164	0.028 *	0.169
diox/oil	spectral	0.128	0.132	0.165 ± 0.003	0.163	0.029 *	0.197
Har	H/100 H	4.3	6.7	3.5 ± 0.2	4.2	7.8 ± 1.0	5.8 ± 0.2
<b>CIRs</b>							
Hart		0.9	1.6	0.6 ± 0.2	0.7	1.5 ± 0.6	1.1 ± 0.2
Hard		1.4	2.2	1.2 ± 0.1	1.0	2.7 ± 0.3	2.0 ± 0.1
Harm		2.1	2.9	1.7 ± 0.0	2.5	3.6 ± 0.1	2.7 ± 0.0
Hbzy		3.4	3.6	3.4 ± 0.3	3.4	7.1 ± 1.3	4.0 ± 0.1
Hbetb		8.5	5.3	7.9 ± 0.6	8.6	9.6 ± 3.3	8.3 ± 0.3
Hbeta		55.1	53.9	64.8 ± 0.1	60.9	48.6 ± 1.1	53.3 ± 0.1
Hgam		28.6	30.5	20.5 ± 0.5	22.9	26.9 ± 2.5	28.7 ± 0.1
<b>CG Train C13</b>							
Lna	atoms	8.1	7.8	10.6 ± 0.0	10.0	8.2 ± 0.0	8.9 ± 0.0
<b>Groups</b>							
Cna	n-Alkane	18.2	17.1	32.6 ± 1.0	28.9	16.4 ± 0.1	19.7 ± 1.4
Cma	Me-Alkane	8.8	7.8	8.1 ± 0.9	11.2	8.2 ± 0.1	8.8 ± 0.1
Ccs	Cyc+Sub	60.6	58.3	44.5 ± 1.3	44.1	50.5 ± 0.9	54.2 ± 1.4
Car	Arom Core	12.5	16.8	14.8 ± 0.6	15.8	24.9 ± 0.7	17.4 ± 0.1
Sum		100.0	100.0	100.0	100.0	100.0	100.0

\* Gravimetric dioxane/oil ratios were varied six-fold for samples of oil V3.

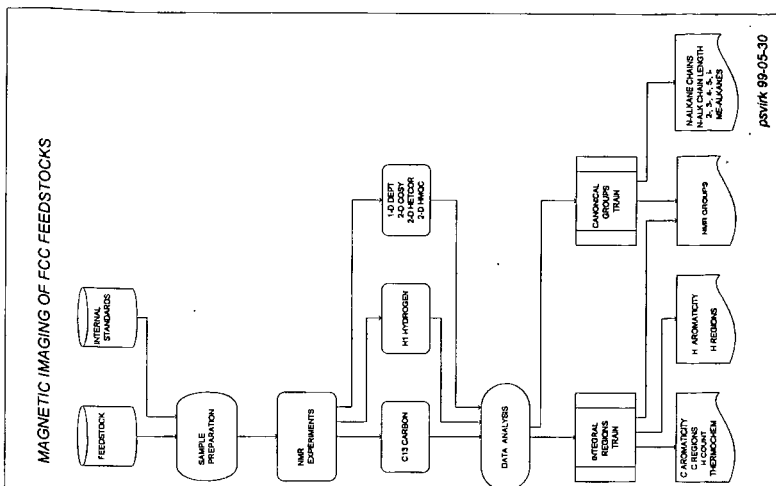


Fig. 1. Magnetic Imaging of FCC Feedstocks.

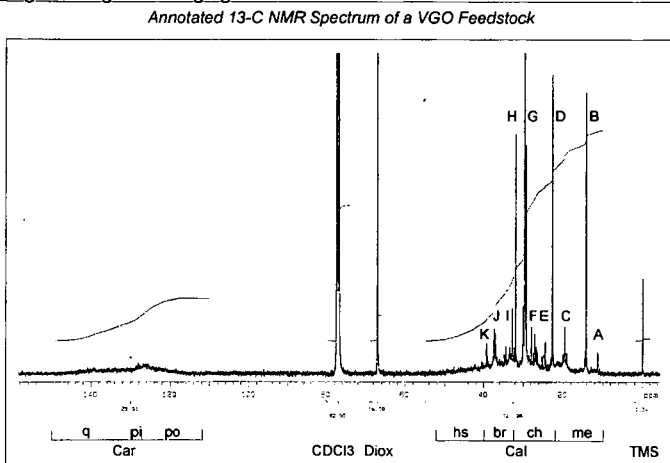


Fig. 2. Annotated 13-C NMR Spectrum of a VGO Feedstock.

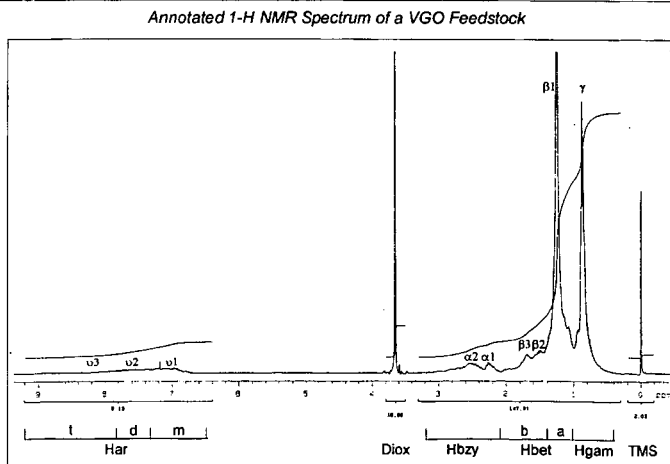


Fig. 3. Annotated 1-H NMR Spectrum of a VGO Feedstock.

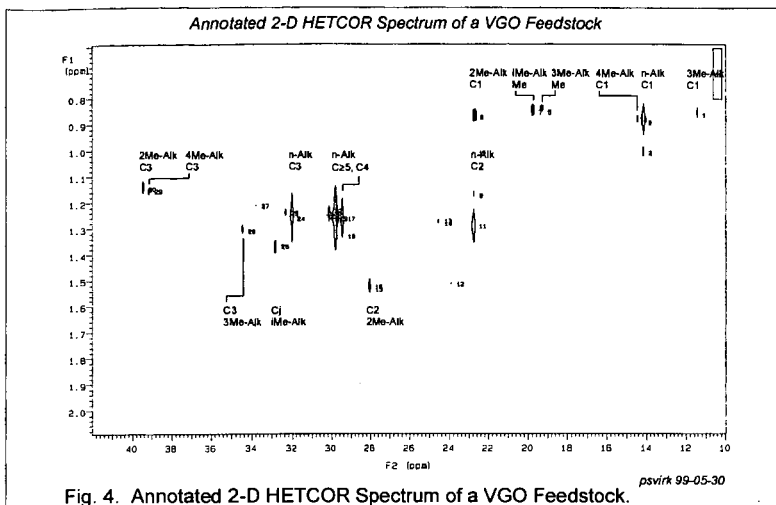


Fig. 4. Annotated 2-D HETCOR Spectrum of a VGO Feedstock.

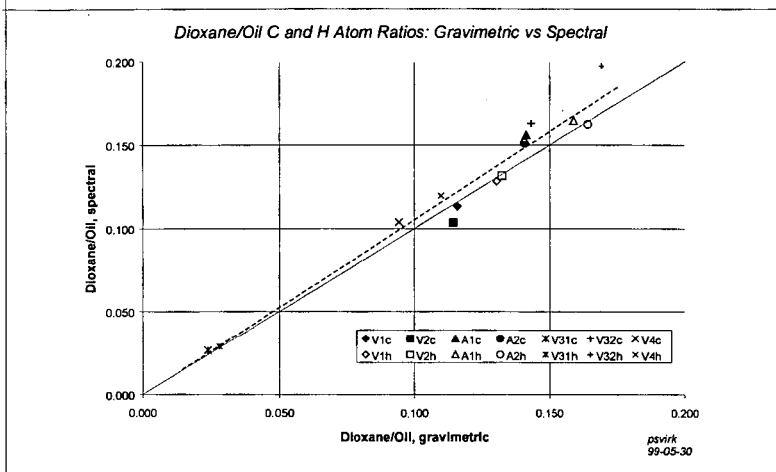


Fig. 5. Dioxane/Oil Ratios of C and H atoms: Gravimetric vs Spectral.

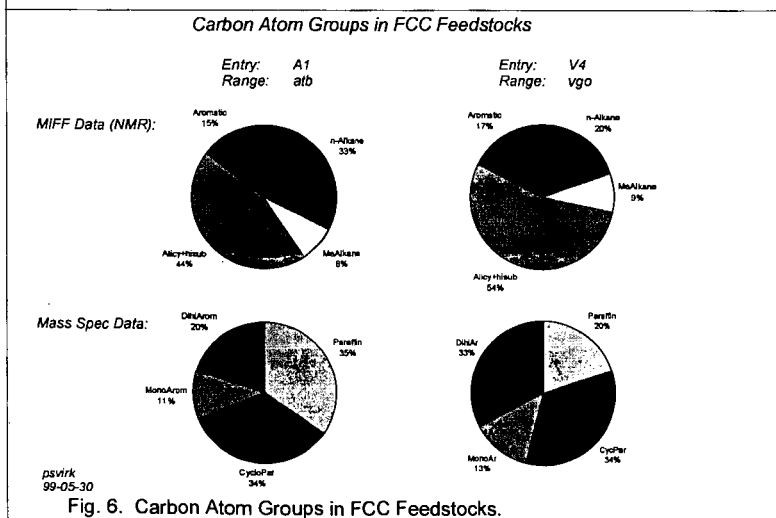
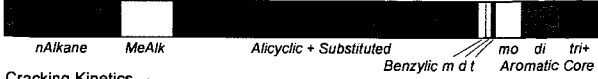


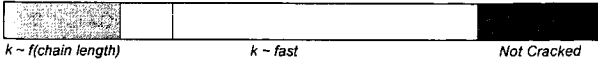
Fig. 6. Carbon Atom Groups in FCC Feedstocks.

## Relation of NMR-Derived Feedstock Characterizations to FCC Performance.

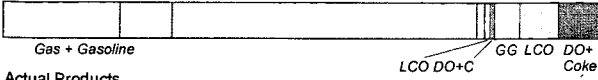
Advanced MIFF Groups



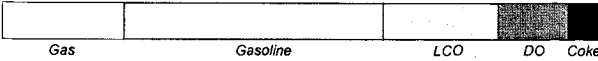
Cracking Kinetics



Potential Products



Actual Products

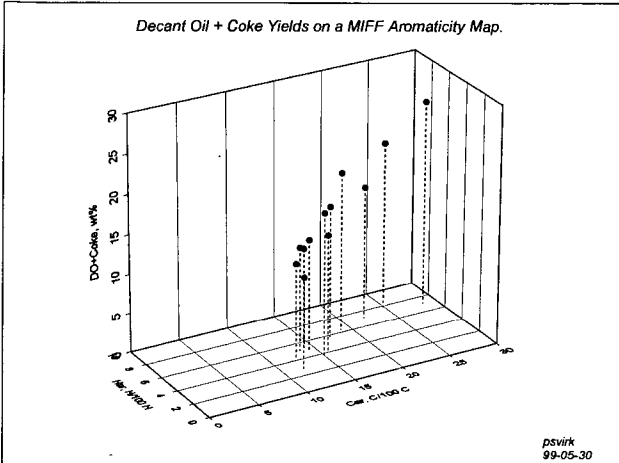


Sample: V4  
Range: vgo

psvirk  
99-05-30

Fig. 7. Relation of NMR-Derived Feedstock Characterizations to FCC Performance.

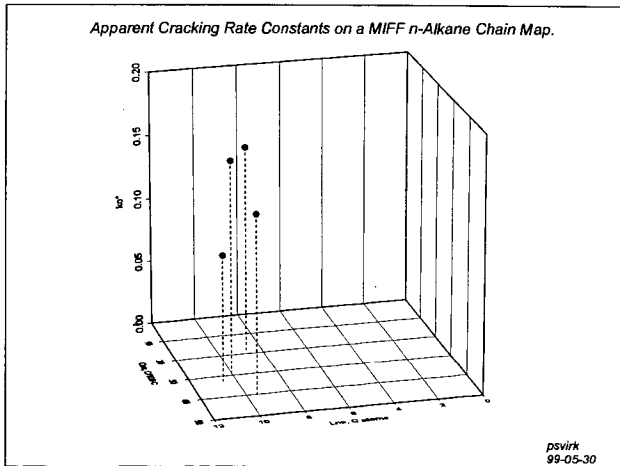
### Decant Oil + Coke Yields on a MIFF Aromaticity Map.



psvirk  
99-05-30

Fig. 8. Decant Oil + Coke Yields on a MIFF Aromaticity Map.

### Apparent Cracking Rate Constants on a MIFF n-Alkane Chain Map.



psvirk  
99-05-30

Fig. 9. Apparent Cracking Rate Constants on a MIFF n-Alkane Chain Map.